Development of a Mathematical Model to Investigate the Effects of Couple and Surface Stresses in Axisymmetric Surface-Loaded

Punyatorn Jhaengkrajhang[1] and Jintara Lawongkerd [2,*]

[1,2]Research Unit in Advanced Mechanics of Solids and Vibration, Department of Civil Engineering, Faculty of Engineering, Thammasat School of Engineering, Thammasat University, Pathumthani 12120, Thailand.

**Corresponding author; E-mail address: ljintara@engr.tu.ac.th.*

Abstract

This research presents a mathematical model for analyzing the mechanical behavior of multilayered nanoscale materials under axisymmetric surface loading. The materials are assumed to be homogeneous, isotropic, and exhibit linear elasticity governed by couple stress and surface stress theories. Hankel integral transforms and stiffness matrices are employed to obtain closed-form solutions for stress, displacement, and couple stress, while incorporating surface stress effects at the surface and interfaces.

The findings indicate that increasing the number of material layers enhances the overall stiffness and reduces surface deformation, particularly in systems with on an elastic half-space. The proposed model provides an effective framework for understanding size-dependent mechanical responses, offering valuable insights for the design and optimization of advanced multilayered coatings in micro- and nanoscale applications.

Keywords: Axisymmetric surface loaded, Linearly elastic multilayer, Couple stress, Surface stress, Size effect

1. Introduction

Multi-layered nanoscale materials, such as nanofilms and multilayered nanostructures, are widely employed in various industries, including electronics, biomedical devices, and aerospace applications [1–2], due to their ability to be engineered with layer-specific mechanical or functional properties tailored to their intended applications. However, classical solid mechanics models are insufficient for accurately capturing the effects of couple stress and surface stress, which become increasingly significant at the nanoscale. To address this limitation, this research focuses on developing a mathematical model to describe the mechanical behavior of multilayered materials under axisymmetric surface loading, based on the Couple Stress Elasticity Theory [3–5] and the Gurtin–Murdoch Surface Elasticity Theory [6–8]. These theoretical frameworks enable the precise evaluation of internal stresses and interfacial surface tension between material layers.

The behavior of multilayered materials at the nanoscale under axisymmetric indentation has been extensively investigated in previous studies. For example, Rungamornrat et al. (2016) examined surface stress effects in a single layer and later extended the model to multilayered systems [9]. Tirapat et al. (2017) analyzed the axisymmetric contact behavior of multilayered materials embedded in an elastic half-space [10], while Tarntira et al. (2019) studied the influence of surface energy on multilayered media using the Gurtin–Murdoch elasticity theory [5]. Furthermore, Intarit et al. (2023) explored functionally graded layers [11], and Wongviboonsin et al. (2022) developed a generalized analytical model for systems with alternating hard-soft layers [12]. More recently, Le et al. (2020, 2021, 2022) proposed models combining couple stress elasticity with Gurtin–Murdoch surface elasticity for multilayered nanoscale systems [13–15]. Additionally, Lawongkerd et al. (2023) introduced a Hankel transform-based analytical solution for thin films on rigid substrates [16].

While these studies have contributed significantly to the field, the integration of both couple stress and surface stress theories into a unified framework for analyzing multilayered materials, particularly under axisymmetric surface loading, remains limited. The present research aims to fill this gap by providing a comprehensive model that more accurately captures size-dependent mechanical behavior and complex interactions at the nanoscale.

2. Theoretical and Methodology

This study develops a mathematical model to analyze multilayered bi-material systems under axisymmetric loading by incorporating couple stress and surface stress theories. The governing equations are formulated using couple stress elasticity for the bulk and Gurtin–Murdoch surface elasticity for the interfaces. Closed-form solutions are obtained via the Hankel transform method for both rigid and elastic substrates.

2.1 Problem Description

Consider a multilayered flexible medium in three dimensions, accounting for the deformation and forces in each layer under external loads, while incorporating the influence of surface energy to study the properties of nanoscale materials. In Figure 1, $\{O;r,\theta,z\}$ there O represents the origin in the coordinate system. The material is assumed to be homogeneous, isotropic, and linearly elastic. The Lame constants $\{\mu_1,\lambda_1,\mu_2,\lambda_2\}$ are determined based on couple stress theory (Mindlin and Tiersten, 1962; Koiter, 1964). The surface components originate from linearly elastic materials following the Gurtin-Murdoch surface elasticity theory, which employs the same Lame constants $\{\mu^s,\lambda^s\}$ the tensile surface forces $\{\tau^s\}$, as described by Gurtin and Murdoch (1975, 1978), act at the center of the surface. The deformation and forces that occur within any layer n are considered, where the radius of the applied force is equal to a.

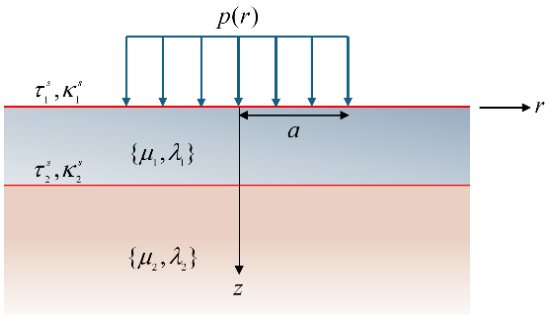

Fig 1. Multilayered three-dimensional coating system under axisymmetric surface loading with surface and interfacial stress effects.

2.2 Couple stress theory

To simulate the elastic response of bulk materials with microstructures, the couple stress theory proposed by Mindlin and Tiersten (1962) and Koiter (1964) is adopted. This theory extends classical elasticity by incorporating the effects of microstructural rotations and couple stresses [3-5], which become significant at smaller scales. The fundamental equations governing the elastic field under axisymmetric deformation with zero body force and couple are presented as follows.

2.2.1 Equilibrium Equations

The equilibrium equations ensuring force balance and moment balance within the material are given by:

$$\frac{\partial\sigma_{rr}}{\partial r}+\frac{\partial\sigma_{zr}}{\partial z}+\frac{\sigma_{rr}-\sigma_{\theta\theta}}{r}=0 \tag{1}$$

$$\frac{\partial\sigma_{rz}}{\partial r}+\frac{\partial\sigma_{zz}}{\partial z}+\frac{\sigma_{rz}}{r}=0 \tag{2}$$

$$\frac{\partial m_{r\theta}}{\partial r}+\frac{\partial m_{z\theta}}{\partial z}+\frac{m_{r\theta}+m_{\theta r}}{r}+\sigma_{zr}-\sigma_{rz}=0 \tag{3}$$

2.2.2 Stress-Strain Relations

The stress components $\{\sigma_{rr},\sigma_{\theta\theta},\sigma_{zz},\sigma_{zr}\}$ relate to strain components $\{\varepsilon_{rr},\varepsilon_{\theta\theta},\varepsilon_{zz},\varepsilon_{zr}\}$ using Lame's constants $\{\mu,\lambda\}$:

$$\sigma_{rr}=2\mu\varepsilon_{rr}+\lambda(\varepsilon_{rr}+\varepsilon_{\theta\theta}+\varepsilon_{zz}) \tag{4}$$

$$\sigma_{\theta\theta}=2\mu\varepsilon_{\theta\theta}+\lambda(\varepsilon_{rr}+\varepsilon_{\theta\theta}+\varepsilon_{zz}) \tag{5}$$

$$\sigma_{zz}=2\mu\varepsilon_{zz}+\lambda(\varepsilon_{rr}+\varepsilon_{\theta\theta}+\varepsilon_{zz}) \tag{6}$$

$$\sigma_{rz}+\sigma_{zr}=4\mu\varepsilon_{rz} \tag{7}$$

These equations describe how stress develops within the material in response to deformation.

2.2.3 Couple Stress Components

In couple stress theory, additional moments exist within the material, governed by:

$$m_{z\theta}=4\eta\kappa_{z\theta},\ m_{\theta z}=4\eta'\kappa_{z\theta} \tag{8}$$

$$m_{r\theta}=4\eta\kappa_{r\theta}+4\eta'\kappa_{\theta r},\ m_{\theta r}=4\eta\kappa_{\theta r}+4\eta'\kappa_{r\theta} \tag{9}$$

where η and η' are material parameters that define the influence of microstructures.

2.2.4 Strain and Curvature Components

Strain components in terms of displacements $\{u_r,u_z\}$:

$$\varepsilon_{rr}=\frac{\partial u_r}{\partial r},\ \varepsilon_{\theta\theta}=\frac{u_r}{r},\ \varepsilon_{zz}=\frac{\partial u_z}{\partial z} \tag{10}$$

$$\varepsilon_{rz}=\varepsilon_{zr}=\frac{1}{2}\left(\frac{\partial u_r}{\partial z}+\frac{\partial u_z}{\partial r}\right) \tag{11}$$

Curvature components related to rotation:

$$\kappa_{z\theta}=\frac{\partial \Omega_\theta}{\partial z},\ \kappa_{\theta r}=-\frac{\Omega_\theta}{r},\ \kappa_{r\theta}=\frac{\partial \Omega_\theta}{\partial r} \tag{12}$$

$$\Omega_\theta=\frac{1}{2}\left(\frac{\partial u_r}{\partial z}-\frac{\partial u_z}{\partial r}\right) \tag{13}$$

where Ω_θ represents the material's rotational effects.

2.3 Surface Stress Theory

A material surface adhered to the top of the bulk is modeled using the surface elasticity theory proposed by Gurtin and Murdoch (1975, 1978). This theory accounts for surface stresses, which play a significant role in nanoscale materials [6-8]. In an axisymmetric case, the non-zero surface displacements $\{u_r^s,u_z^s\}$, surface strains $\{\varepsilon_{rr}^s,\varepsilon_{zz}^s\}$ and surface stresses $\{\sigma_{rr}^s,\sigma_{\theta\theta}^s,\sigma_{rz}^s\}$ are governed by the following equations.

2.3.1 Governing Equations

The equilibrium equations ensuring force balance on the surface are given by:

$$\frac{d\sigma_{rr}^s}{dr}+\frac{\sigma_{rr}^s-\sigma_{\theta\theta}^s}{r}+t_r^s+q(r)=0 \tag{14}$$

$$\frac{d\sigma_{rz}^s}{dr}+\frac{\sigma_{rz}^s}{r}+t_z^s+p(r)=0 \tag{15}$$

where t_r^s,t_z^s are the radial and vertical tractions acting on the surface due to the underlying bulk layer.

2.3.2 Surface Stress-Strain Relations

The surface stress components $\{\sigma_{rr}^s,\sigma_{\theta\theta}^s,\sigma_{rz}^s\}$ are related to the surface strain components $\{\varepsilon_{rr}^s,\varepsilon_{zz}^s\}$ and the residual surface tension τ^s as follows:

$$\sigma_{rr}^s=\tau^s+(2\mu^s+\lambda^s)\varepsilon_{rr}^s+(\mu^s+\lambda^s)\varepsilon_{\theta\theta}^s \tag{16}$$

$$\sigma_{\theta\theta}^s=\tau^s+(2\mu^s+\lambda^s)\varepsilon_{\theta\theta}^s+(\mu^s+\lambda^s)\varepsilon_{rr}^s \tag{17}$$

$$\sigma_{rz}^s=\tau^s\frac{du_z^s}{dr} \tag{18}$$

where $\{\mu^s,\lambda^s\}$ are the surface Lame constants.

2.3.3 Surface Strain Components

The surface strains are expressed in terms of surface displacements $\{u_r^s,u_z^s\}$ as follows:

$$\varepsilon_{rr}^s=\frac{du_r^s}{dr},\quad \varepsilon_{\theta\theta}^s=\frac{u_r^s}{r} \tag{19}$$

2.3.4 Equilibrium Equations in Terms of Surface Displacements

By combining Eqs. (14)–(19), the equilibrium equations can be rewritten in terms of the surface displacements as follows:

$$\kappa^s\left(\frac{d^2u_r^s}{dr^2}+\frac{1}{r}\frac{du_r^s}{dr}-\frac{u_r^s}{r^2}\right)+t_r^s+q(r)=0 \tag{20}$$

$$\tau^s\left(\frac{d^2u_z^s}{dr^2}+\frac{1}{r}\frac{du_z^s}{dr}\right)+t_z^s+p(r)=0 \tag{21}$$

where $\kappa^s=2\mu^s+\lambda^s$, and it is assumed that the residual surface tension τ^s is spatially independent.

2.4 Solution of the Boundary Conditions

In solving the problem of forces acting on a multilayered medium with axisymmetric properties, the resulting displacement, force stress, and couple stress consider materials with homogenous, isotopic, and linearly elastic. The surfaces are perfectly bonded, and there are normal forces traction $p(r)$, shear forces traction $q(r)$, and couple traction $m(r)$.

$$\sigma_{zz}^1|_{z=0}+\tau_1^s\left(\frac{d^2u_z^s}{dr^2}+\frac{1}{r}\frac{du_z^s}{dr}\right)\Bigg|_{z=0}+p(r)=0 \tag{22}$$

$$\sigma_{zr}^1|_{z=0}+\kappa_1^s\left(\frac{d^2u_r^s}{dr^2}+\frac{1}{r}\frac{du_r^s}{dr}-\frac{u_r^s}{r^2}\right)\Bigg|_{z=0}+q(r)=0 \tag{23}$$

$$m_{z\theta}^1|_{z=0}+m(r)=0 \tag{24}$$

Because every layer is perfectly bonded at the interface between the top and bottom layers, the rigid substrate of the bottommost layer prevents it from rotating or translating. When

considering any layer $n = 1,2,3,...,N$ and N is a total number of layers.

$$u_r^{n-1}\Big|_{z=h_n} = u_r^n\Big|_{z=h_n} \tag{25}$$

$$u_z^{n-1}\Big|_{z=h_n} = u_z^n\Big|_{z=h_n} \tag{26}$$

$$\Omega_\theta^{n-1}\Big|_{z=h_n} = \Omega_\theta^n\Big|_{z=h_n} \tag{27}$$

$$\sigma_{zz}^{n-1}\Big|_{z=h_n} = \sigma_{zz}^n\Big|_{z=h_n} + \tau_n^s\left(\frac{d^2u_z}{dr^2}+\frac{1}{r}\frac{du_z}{dr}\right)\Big|_{z=h_n} \tag{28}$$

$$\sigma_{zr}^{n-1}\Big|_{z=h_n} = \sigma_{zr}^n\Big|_{z=h_n} + \kappa_n^s\left(\frac{d^2u_r}{dr^2}+\frac{1}{r}\frac{du_r}{dr}-\frac{u_r}{r^2}\right)\Big|_{z=h_n} \tag{29}$$

$$m_{z\theta}^{n-1}\Big|_{z=h_n} = m_{z\theta}^n\Big|_{z=h_n} \tag{30}$$

$$u_r\Big|_{z=h_N} = 0 \tag{31}$$

$$u_z\Big|_{z=h_N} = 0 \tag{32}$$

$$m_{z\theta}^N\Big|_{z=h_N} = 0 \tag{33}$$

To obtain the closed-form solution for the elastic field in a multilayered medium, a method based on the Hankel Transform is employed, incorporating the displacement field representation for each layer. The system is considered under axisymmetric surface loading, where the vertical and radial displacements in the multilayered structure are given by:

$$u_r = -\frac{\partial}{\partial r}\left[\ell^2\frac{\partial\Psi}{\partial z}+\alpha\left\{z\left(1-\ell^2\Delta\right)\Psi+\Phi\right\}\right] \tag{34}$$

$$u_z = \Psi-\ell^2\frac{\partial^2\Psi}{\partial z^2}-\alpha\frac{\partial}{\partial z}\left\{z\left(1-\ell^2\Delta\right)\Psi+\Phi\right\} \tag{35}$$

Where $\alpha = (\lambda+\mu)/2(\lambda+2\mu)$ represents the Lame parameters, $\ell = \sqrt{\eta/\mu}$ denotes the characteristic length scale related to couple stress effects. $\Psi(r,z)$ and $\Phi(r,z)$ are unknown displacement potential functions to be determined. Δ is the Laplacian operator in cylindrical coordinates, which accounts for the radial and vertical displacement effects. The governing equations for each layer follow:

$$(1-\ell^2\Delta)\Delta\Psi = 0\,,\quad \Delta\Phi = 0 \tag{36}$$

By applying the Hankel Transform, the general solutions for $\Psi(r,z)$ and $\Phi(r,z)$ are expressed as:

$$\Psi(r,z) = \int_0^\infty \begin{Bmatrix} C_1e^{-\xi(t-z)}+C_2e^{-\xi z} \\ +C_3e^{-\zeta(t-z)/\ell}+C_4e^{-\zeta z/\ell}\end{Bmatrix} J_0(\xi r)\xi d\xi \tag{37}$$

$$\Phi(r,z) = \int_0^\infty \left\{C_5e^{-\xi(t-z)}+C_6e^{-\xi z}\right\}J_0(\xi r)\xi d\xi \tag{38}$$

Where J_0 is the Bessel function of the first kind, often used in axisymmetric problems. ξ is the transform parameter from Hankel Transform. $\zeta = \sqrt{1+\ell^2\xi^2}$ is a parameter incorporating couple stress effects. $C_i\,(i=1,2,...,6)$ are unknown coefficients to be determined from boundary conditions. The general solution of the displacements $\{u_r,u_z\}$, the rotation $\{\Omega_\theta\}$, the force stress component $\{\sigma_{rr},\sigma_{\theta\theta},\sigma_{zz},\sigma_{zr}\}$, and the couple stress components $\{m_{r\theta},m_{\theta r},m_{z\theta},m_{\theta z}\}$ can be obtained upon substitution of Eqs. (37) and (38) into Eqs. (34), (35) and (4)-(13). The explicit expressions for the complete elastic field within the bulk layer, in term of the unknown coefficients $C_i\,(i=1,2,...,6)$.

By enforcing the boundary conditions given by Eqs. (22)-(33) together with the general solution for $\{u_r,u_z,\sigma_{zz},\sigma_{zr},m_{z\theta}\}$ a system of linear algebraic equations is obtained for determining the coefficients $C_i^n\,(i=1,2,...,6)$:

$$K(\xi)C = F(\xi) \tag{39}$$

Where C are the coefficient matrix and the vector $F(\xi)$ are given explicitly by

$$C = \begin{bmatrix} C_1^1 & C_2^1 & C_3^1 & C_4^1 & C_5^1 & C_6^1 & \cdots & C_6^N\end{bmatrix}_{6N}^T \tag{40}$$

$$F(\xi) = \begin{bmatrix} P(\xi) & Q(\xi) & M(\xi) & 0 & 0 & 0 & \cdots & 0\end{bmatrix}_{6N}^T \tag{41}$$

Where

$$P(\xi) = -\int_0^\infty p(r)J_0(\xi r)rdr \tag{42}$$

$$Q(\xi) = -\int_0^\infty q(r) J_1(\xi r) r dr \tag{43}$$

$$M(\xi) = -\int_0^\infty m(r) J_1(\xi r) r dr \tag{44}$$

The stiffness matrix of the multilayer K_{ij}^n can be assembled by applying the continuity condition of traction at any layer $n = 1, 2, 3, ..., N$, which can be expressed as follows:

$$K(\xi) = \begin{Bmatrix} K_{3\times6}^1 & 0 & 0 & 0 & 0 & 0 \\ K_{6\times6}^1 & K_{6\times6}^2 & 0 & 0 & 0 & 0 \\ 0 & \ddots & \ddots & 0 & 0 & 0 \\ 0 & 0 & K_{6\times6}^{n-1} & K_{6\times6}^n & 0 & 0 \\ 0 & 0 & 0 & \ddots & \ddots & 0 \\ 0 & 0 & 0 & 0 & K_{6\times6}^{N-1} & K_{6\times6}^N \\ 0 & 0 & 0 & 0 & 0 & K_{3\times6}^N \end{Bmatrix}_{6N\times6N} \tag{45}$$

When matrix $K_{3\times6}^1$ and $K_{3\times6}^N$ represents the equation for the top and bottommost surface, $K_{6\times6}^n$ represent the equation at the interface between layers. The solution of the system (Eqs. (39)) for each $\xi \in [0, \infty)$ can be obtained numerically via standard linear solvers. Once $C_i^n (i = 1, 2, ..., 6)$ are solved, the elastic field within the bulk layer.

3. Result and Discussion

To investigate the mechanical behavior of a multilayered system subjected to a uniformly distributed load $p_0 / 2\mu$, the analysis is categorized into four models. Model-1 considers the combined effects of couple stress and surface stress, while Model-2 takes into account only the influence of surface stress. Model-3 focuses solely on the effects of couple stress, and Model-4 represents the classical elasticity case, in which neither couple stress nor surface stress is considered. To facilitate the formulation and interpretation of results, the following normalized coordinates and parameters are introduced: $\bar{r} = r / \Lambda$, $\bar{z} = z / \Lambda$, $\overline{h_i} = h_i / \Lambda$, $\overline{\tau_i^s} = \tau_i^s / 2\mu_1 \Lambda$ and $l_0 = \ell / \Lambda$ with $\Lambda = \kappa_1^s / 2\mu_1$ denoting the length scale of the material surface are introduced.

3.1 Verifycation

To verify the correctness of the governing equations presented in Section 2, comparisons were made with relevant existing studies. The first validation was performed against the classical two-layer solution presented by Gerrard (1969), corresponding to Model 4. Additionally [17], the results were compared with those reported by Rungamornrat et al. (2016), which investigated the influence of surface stress in a single-layer configuration (Model-2 and Model-4) [9], and by Lawongkerd et al. (2023), which considered both couple stress and surface stress effects in a single-layer system [16]. The resulting normalized vertical stress σ_{zz} / p_0 shows excellent agreement with all reference solutions, as illustrated in Fig. 2.

To more realistically investigate the size-dependent behavior and effects, the present study advances beyond previous models by considering a bi-material coating system, which more accurately reflects practical and complex configurations observed in real-world applications.

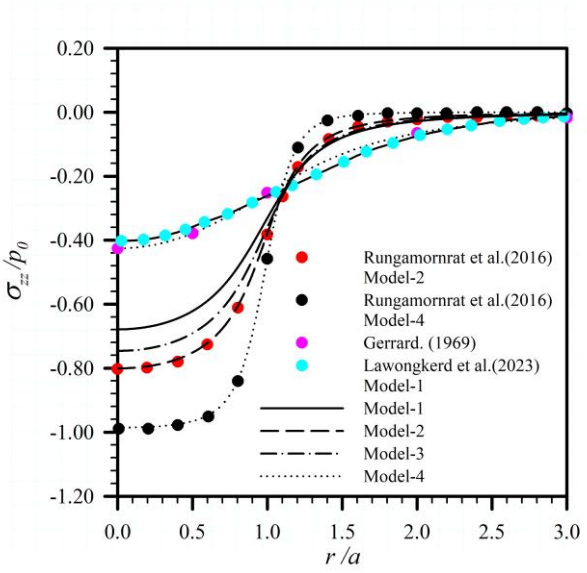

Fig 2. Verification of normalized vertical stress with reference solutions from the literature.

3.2 Bi-material coating

In this section, the mechanical behavior of a bi-material coating system is investigated, considering two configurations: a bi-material layer deposited on a rigid substrate and a bi-material layer bonded to an elastic half-space, as illustrated in Figs. 3a and 3b, respectively. The material parameters used in the analysis correspond to the upper layer being aluminum Al[111], with $\mu = 26.13 \times 10^9 N/m^2$ and $\lambda = 58.17 \times 10^9 N/m^2$, as reported by Miller and Shenoy (2000) [18], and the lower layer being silicon Si[100], also with $\mu = 40.2256 \times 10^9 N/m^2$ and $\lambda = 78.0849 \times 10^9 N/m^2$, as reported by Meyers and

Chawla (2008) [19]. The thickness of each material layer is denoted as h_S for Al[111] and h_H for Si[100], and the total thickness of a single bi-material cycle is defined as $n_C = h_S + h_H$. The total thickness of the bi-material composite system is represented by H.

To investigate the behavior of bi-material coating systems, vertical stress at the location $\bar{z}/\bar{H} = 1.0$ is analyzed under increasing numbers of bi-material layers $n_C = \{1, 2, 4, 8, 16, 32, 64\}$ for Model-1, with the parameters set as $\bar{H}/\bar{a} = 1.0$, $\bar{a} = 1.0$ and $l_0 = 1.0$. The surface stress effects of the topmost layer are defined as $\tau_1^s = 1 N/m$ $\kappa_1^s = 6.0991 N/m$, while for all bi-material interfaces, the surface stress ratios are specified as $\bar{\tau}_2^s / \bar{\tau}_1^s = 2.0$ and $\bar{\kappa}_2^s / \bar{\kappa}_1^s = 2.0$. The configuration of the bi-material coating on a rigid substrate is illustrated in Fig. 4, whereas the bi-material on an elastic half-space is shown in Fig. 5, with the elastic half-space defined by $E = 76GPa$ and $v = 0.3$.

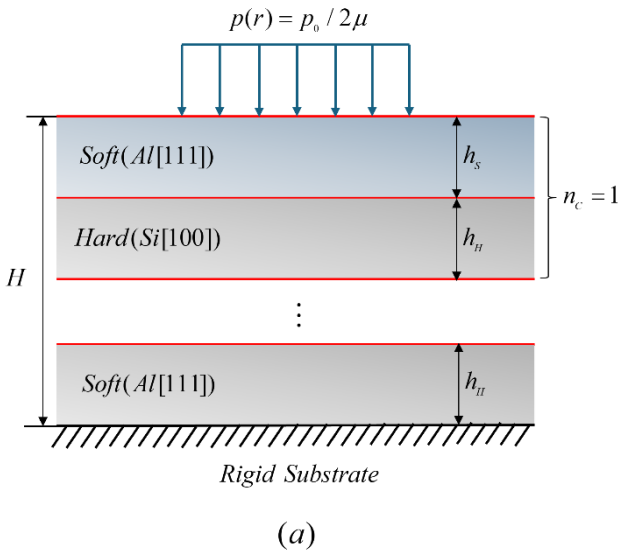

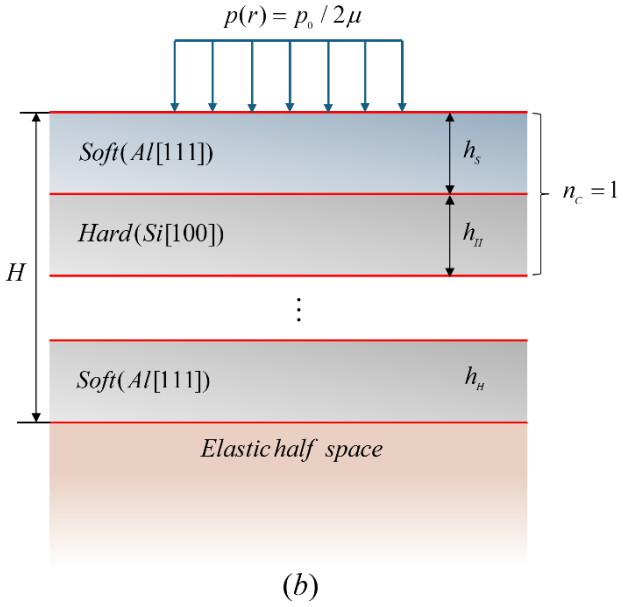

Fig 3. Multilayered bi-material coating systems under axisymmetric surface loading: (a) on a rigid substrate and (b) on an elastic half-space.

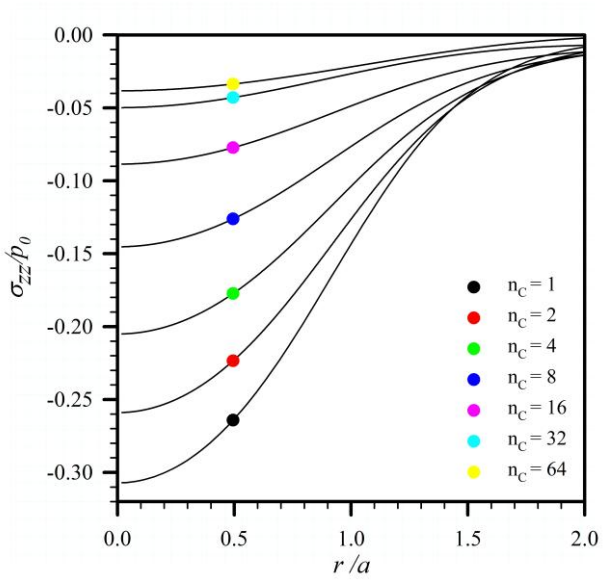

Fig 4. Normalized vertical stress at $\bar{z}/\bar{H} = 1.0$ for multilayered bi-material systems on a rigid substrate with varying number of layers n_C.

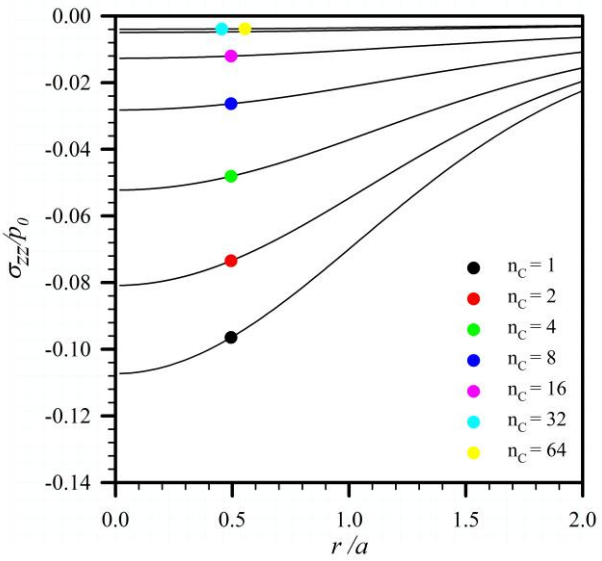

Fig 5. Normalized vertical stress at $\bar{z}/\overline{H} = 1.0$ for multilayered bi-material systems on an elastic half-space with varying number of layers n_C.

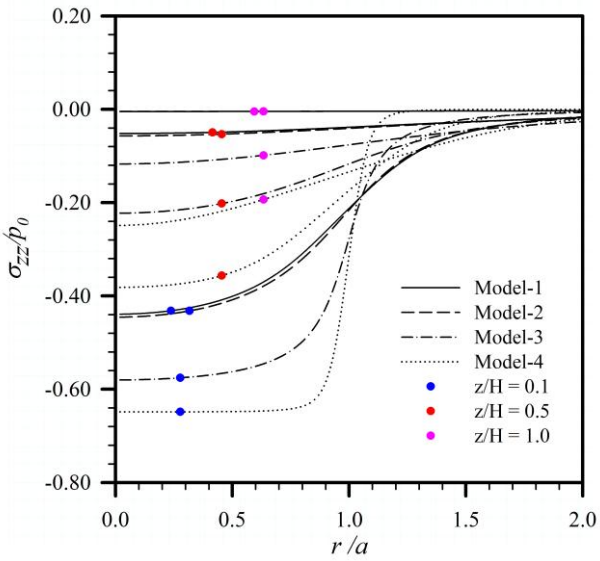

Fig 6. Normalized vertical stress σ_{zz}/p_0 distribution along r/a at different depths $\bar{z}/\overline{H} = \{0.1, 0.5, 1.0\}$ for all four models.

When comparing the normalized vertical stress in Figs. 4 and 5, it is evident that for the same number of layers n_C, the vertical stress in the bi-material on the rigid substrate is significantly higher in all cases. This is attributed to the resistance to deformation provided by the rigid substrate. Moreover, as n_C increases, the system exhibits a greater ability to resist vertical deformation due to the increasingly dominant influence of surface stresses. To further investigate the coating behavior for optimal performance, the case of bi-material on an elastic half-space with $n_C = 32$ is selected for detailed analysis of the elastic field within the bi-material structure. This configuration is considered to more realistically represent the behavior of coating systems compared to those on a rigid substrate.

Figs. 6–8 present the elastic field behavior at normalized depths $\bar{z}/\overline{H} = \{0.1, 0.5, 1.0\}$ for all four models. As shown in Fig. 6, the normalized vertical stress σ_{zz}/p_0 in Model-1 and Model-2 is significantly lower than in Model-3 and Model-4, primarily due to the dominant influence of surface stress effects at the material interfaces. Notably, at $\bar{z}/\overline{H} = 0.1$, σ_{zz}/p_0 approaches zero, highlighting the strong suppression of vertical stress near the surface caused by interfacial surface stresses.

In Fig. 7, the normalized vertical displacement u_z/Λ indicates that Model-4 (classical elasticity) exhibits the largest deformation. In contrast, the presence of surface stress between layers in Model-1 and Model-2 contributes to the suppression of deformation, effectively enhancing the overall stiffness of the bi-material system.

In Fig. 8, the normalized couple stress component is presented. The results for Model-2 and Model-4 are identically zero in all cases, both in terms of radial position and depth, as these models do not incorporate couple stress effects in their formulations. This clearly indicates that the presence of couple stress observed in other models arises solely from the inclusion of couple stress theory. In contrast, Model-1 and Model-3, which incorporate couple stress effects, show evidently non-zero values of $m_{\theta r}/p_0\Lambda$. Notably, Model-1, which also includes surface stress effects, exhibits slightly lower values of $m_{\theta r}$ compared to Model-3, indicating that surface stresses at the

material interfaces contribute to suppressing the intensity of the couple stress. Furthermore, it is observed that in both Model-1 and Model-3, the magnitude of the couple stress decreases with increasing depth, demonstrating that the influence of couple stress is most significant near the surface and gradually diminishes deeper into the material. This trend is consistent with the fundamental characteristics of couple stress theory, which accounts for microstructural effects that are particularly dominant in regions near the applied surface load.

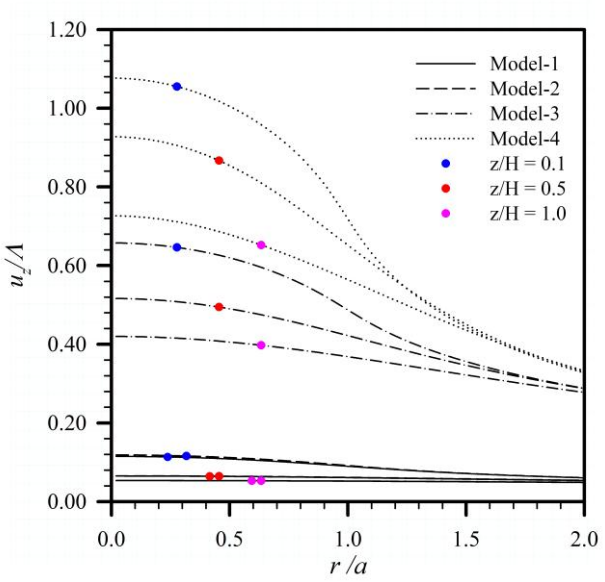

Fig 7. Normalized vertical displacement u_z / Λ distribution along r / a at different depths $\bar{z} / \bar{H} = \{0.1, 0.5, 1.0\}$ for all four models.

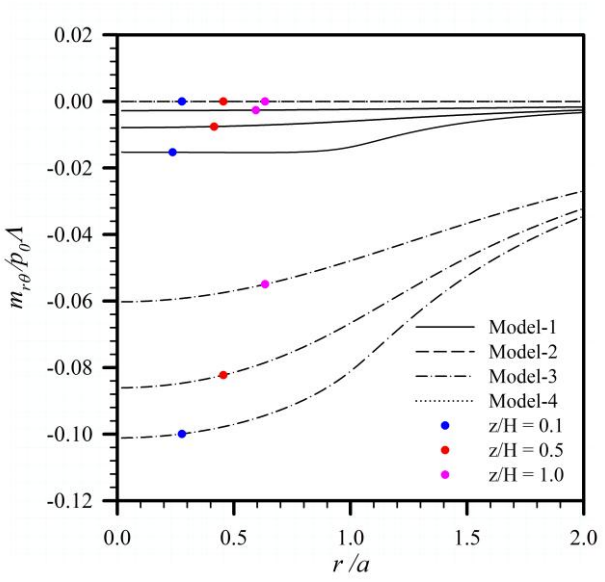

Fig 8. Normalized couple stress $m_{\theta r} / p_0 \Lambda$ distribution along r / a at different depths $z / H = \{0.1, 0.5, 1.0\}$ for all four models.

4. Conclusions

This research highlights the critical roles of couple stress and surface stress in governing the mechanical behavior of multilayer and bi-material coating systems at the nano- and microscale. Through a comprehensive investigation based on couple stress theory and Gurtin–Murdoch surface elasticity, it is demonstrated that the inclusion of these non-classical effects significantly alters the predicted stress and displacement fields compared to classical elasticity models. In particular, surface stress effects are shown to dominate near interfaces, enhancing the overall stiffness and suppressing deformation, while couple stress contributes to size-dependent behaviors that are especially pronounced in regions close to the applied surface loads.

The results further reveal that for multilayered and bi-material systems, especially those with a high number of repeating layers, the accumulation of surface and couple stress effects leads to substantial resistance against vertical deformation. This effect is especially evident in systems deposited on rigid substrates, though it also plays a crucial role in elastic half-space configurations, ensuring more realistic simulations. These findings confirm that accurate modeling of coating systems at small scales must incorporate both surface and couple stress effects in order to capture the true mechanical response. Moreover, the insights gained from this study provide valuable guidance for the design and optimization of advanced coatings in micro/nanoscale engineering applications.

Acknowledgement

The authors would like to express their sincere gratitude to the Research Unit in Advanced Mechanics of Solids and Vibration by Asst. Prof. Dr. Jintara Lawongkerd for their support and contributions to this work. Thank you for your cooperation in strictly following the writing regulations.

References

[1] Khadem, M., Penkov, O. V., Yang, H. K., & Kim, D. E. (2017). Tribology of multilayer coatings for wear reduction: A review. Friction, 5, 248-262.

[2] Surendiran, A., Sandhiya, S., Pradhan, S. C., & Adithan, C. (2009). Novel applications of nanotechnology in medicine. Indian Journal of Medical Research, 130(6), 689-701.

[3] Mindlin, R. D., & Tiersten, H. (1962). Effects of couple-stresses in linear elasticity. Archive for Rational Mechanics and analysis, 11(1), 415-448.

[4] Mindlin, I. A. (1963). Free elastic waves on the surface of a tube of infinite thickness. Journal of Applied Mathematics and Mechanics, 27(3), 823-828.

[5] Koiter, W. (1969). Couple-stresses in the theory of elasticity, I & II.

[6] Gurtin, M. E., & Ian Murdoch, A. (1975). A continuum theory of elastic material surfaces. Archive for rational mechanics and analysis, 57, 291-323.

[7] Gurtin, M. E., & Murdoch, A. I. (1978). Surface stress in solids. International journal of Solids and Structures, 14(6), 431-440.

[8] Gurtin, M. E., Weissmüller, J., & Larche, F. (1998). A general theory of curved deformable interfaces in solids at equilibrium. Philosophical Magazine A, 78(5), 1093-1109.

[9] Rungamornrat, J., Tuttipongsawat, P., & Senjuntichai, T. (2016). Elastic layer under axisymmetric surface loads and influence of surface stresses. Applied Mathematical Modelling, 40(2), 1532-1553.

[10] Tirapat, S., Senjuntichai, T., & Rungamornrat, J. (2017). Influence of surface energy effects on elastic fields of a layered elastic medium under surface loading. Advances in Materials Science and Engineering, 2017(1), 7530936.

[11] Intarit, P. I., Tarntira, K., Senjuntichai, T., & Keawsawasvong, S. (2023). Axisymmetric loading on nanoscale multilayered media. Frontiers of Structural and Civil Engineering, 17(1), 152-164.

[12] Wongviboonsin, W., Le, T. M., Lawongkerd, J., Gourgiotis, P. A., & Rungamornrat, J. (2022). Microstructural effects on the response of a multi-layered elastic substrate. International Journal of Solids and Structures, 241, 111394.

[13] Le, T. M., Bui, T. Q., Lawongkerd, J., Limkatanyu, S., & Rungamornrat, J. (2020). Frictionless contact on elastic half plane with influence of surface and couple stresses. Applied Mechanics and Materials, 897, 73-77.

[14] Le, T. M., Lawongkerd, J., Bui, T. Q., Limkatanyu, S., & Rungamornrat, J. (2021). Elastic response of surface-loaded half plane with influence of surface and couple stresses. Applied Mathematical Modelling, 91, 892-912.

[15] Le, T. M., Wongviboonsin, W., Lawongkerd, J., Bui, T. Q., & Rungamornrat, J. (2022). Influence of surface and couple stresses on response of elastic substrate under tilted flat indenter. Applied Mathematical Modelling, 104, 644-665.

[16] Lawongkerd, J., Le, T. M., Wongviboonsin, W., Keawsawasvong, S., Limkatanyu, S., Van, C. N., & Rungamornrat, J. (2023). Elastic solution of surface loaded layer with couple and surface stress effects. Scientific Reports, 13(1), 1033.

[17] Gerrard, C. M. (1969). Tables of stresses, strains and displacements in two-layer elastic systems under various traffic loads.

[18] Miller, R. E., & Shenoy, V. B. (2000). Size-dependent elastic properties of nanosized structural elements. Nanotechnology, 11(3), 139.

[19] Meyers, M. A., & Chawla, K. K. (2008). Mechanical behavior of materials. Cambridge university press.